

# Cavitation in trees and the hydraulic sufficiency of woody stems

M. Tyree

Department of Botany, University of Vermont, Burlington, VT 05405, and Northeastern Forest Experiment Station, P.O. Box 968, Burlington, VT 05402, U.S.A.

## Introduction

The cohesion theory of sap ascent (Dixon, 1914) forms the basis of our current understanding of the mechanism of water transport in the xylem of plants. Evaporation from cell wall surfaces in the leaf causes the air-water interface to retreat into the fine porous spaces between cellulose fibers in the wall. Capillarity (a consequence of surface tension) tends to draw the interface back up to the surface of the pores and places the mass of water behind it under negative pressure. This negative pressure is physically equivalent to a tension (a pulling force) transmitted to soil water by a continuous water column; any break in the column necessarily disrupts water flow.

In xylem, a break in the water column is induced by a cavitation event, and the xylem of woody plants is highly vulnerable to such events (Tyree and Sperry, 1989). The potential exists for a dynamic cycle of water stress leading to loss of hydraulic conductance and further dynamic stress (see Fig. 1). Transpiration produces dynamic water stress because of the pressure gradient required to maintain sap flow

over the viscous drag in the xylem conduits (tracheids or vessels). The water stress, manifested as a negative pressure, will cause cavitation events – rapid breaks in the water column in a conduit followed by rapid ( $1 \mu s$ ) stress relaxation. Within a few ms, this will result in a water vapor-filled conduit. The water vapor-filled void normally expands to fill only the confines of the conduit in which the cavitation has

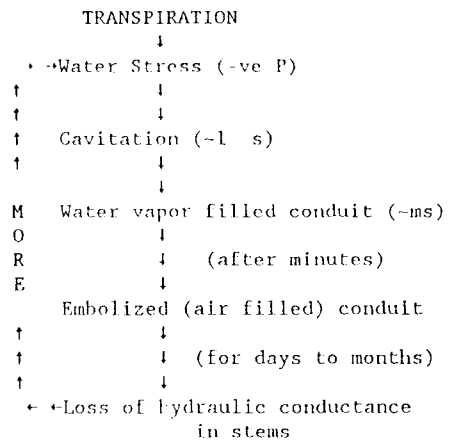


Fig. 1. The 'embolism cycle'

occurred because of the surface tension effects at pit membranes between conduits (Bailey, 1916). Over a period of minutes, an air embolism forms in the cavitating conduit, as gas molecules come out of solution from surrounding water-filled cells. Built-in pathway redundancy ensures that water conduction can continue, despite limited numbers of cavitations. But each embolism will cause a small loss of hydraulic conductance in the stem. A loss of conductance means that sap will have to overcome a larger viscous drag to maintain the same transpiration rate, thus resulting in more water stress. The cycle of events in Fig. 1 is what I call an 'embolism cycle'. A number of important questions can be asked about this cycle. Is it inherently stable or unstable? (In a stable embolism cycle, a plant can sustain a limited amount of embolism and still maintain normal levels of transpiration without further embolism.) How much redundancy is built into the xylem of trees? In other words, how much embolism is too much, thus making the embolism cycle unstable and leading to 'runaway embolism'?

Recently, Tyree and Sperry (1988) attempted to answer these questions by measuring and calculating what might be called the 'hydraulic sufficiency' of trees. In valuing hydraulic sufficiency, 5 steps were used and were repeated for 4 different species: 1) measure the field extremes in evaporative flux from leaves,  $E$ , and field extremes in leaf water potential,  $\psi$ ; 2) quantify the hydraulic architecture of branches by measuring the hydraulic conductance of stems *versus* the diameter of a tree and relate these measures to the amount of foliage supported by each stem; 3) measure the vulnerability of stems to embolism by measuring a curve of loss in hydraulic conductance *versus*  $\psi$  during a dehydration; 4) make a hydraulic map of representative branches or small trees, by cutting a branch into

several hundred stem segments, recording the length, diameter and leaf area attached to each segment, with a numbering system showing the interconnection of the segments; 5) calculate the dynamics of  $\psi$  development and embolism in branches under different transpiration regimes.

Calculations previously published (Tyree and Sperry, 1988) were based on a steady-state model of water flow through a branched catena, so no account was taken of the water storage capacity of leaves and stems or of the temporal dynamics of evaporation. This paper presents results from a more realistic, non-steady-state model on a 10 m tall cedar tree (*Thuja occidentalis* L.). A brief review of the conclusions of the steady-state model and the data used will aid in the understanding of the more advanced model presented here.

### Overview of the steady-state model

'Hydraulic architecture', as used by Zimmermann (1978), describes the relationship of hydraulic conductance of the xylem in various parts of a tree and the amount of leaves it must supply. This is quantified by the leaf specific conductance ( $LSC$ ) – defined as the hydraulic conductance of a stem segment ( $k_h$  = flow rate per unit pressure gradient) divided by the leaf area supplied. This definition allows a quick estimate of pressure gradients in stems. If the  $E$  is about the same throughout a tree, then the xylem pressure gradient ( $dP/dx$ ) in any branch can be estimated from:  $dP/dx = E/LSC$ .

The  $LSC$  of minor branches, 1 mm diameter, is about 30 times less than that of major stems 150 mm diameter in cedar trees (Tyree *et al.*, 1983). Consequently, most of the water potential drop in the

xylem occurs in the small branches and twigs; of the drop in  $\psi$  from the soil to the leaves, about 55% occurs in branches less than 10 mm diameter, about 35% from the larger branches and bole, and 15% in the roots (Tyree, 1988). The same hydraulic architecture is observed in other species (Tyree and Sperry, 1989) and this led Zimmermann (1983) to propose the 'segmentation hypothesis' to explain the value of decreasing *LSC* along with decreasing stem diameter. Embolism potentially can occur throughout the tree and, by decreasing the xylem conductance, can substantially influence water status. According to the segmentation hypothesis, embolism will preferentially occur in minor branches where *LSC*s are lowest and consequent xylem tensions are greatest. Under severe water stress conditions, peripheral parts of the tree would be sacrificed and the trunk and main branches (where most of the carbon investment has occurred) would remain functional and permit regrowth. Another important consequence of the hydraulic architecture is the hydraulic resistance to water flow from the ground level to all minor branches, which is *approximately* the same for all twigs, whether the twig is located near the base of a crown and at the end of a short hydraulic path or at the top of a crown and at the end of a long

hydraulic path. All shoots are approximately equally capable of competing for the water resources of the tree. Trees that show strong apical dominance are the exception. In these trees, the *LSC* remains high or increases towards the dominant apex (Ewers and Zimmermann, 1984a, b).

The vulnerability curve (see Fig. 2A) used in model calculations was obtained under laboratory conditions by dehydrating cedar branches to known water potentials and then measuring the resulting loss of hydraulic conductance by methods described elsewhere (Sperry *et al.*, 1987). The hydraulic conductivity data are shown as a log-log plot (see Fig. 2B) of conductance *versus* stem diameter.

Information on the hydraulic sufficiency of cedar was derived by writing a computer model that calculated the  $\psi$ 's that must develop in different parts of a 2.6 m sapling under steady-state conditions, that is, when water flow through each stem segment ( $\text{kg}\cdot\text{s}^{-1}$ ), equaled the evaporation rate ( $\text{kg}\cdot\text{s}^{-1}$ ) from all leaves supplied by the stem segment. To do this, the computer model needed an input data set that amounted to a 'hydraulic map' of the sapling cut into several hundred segments. Each segment was numbered and then coded to show which segment its

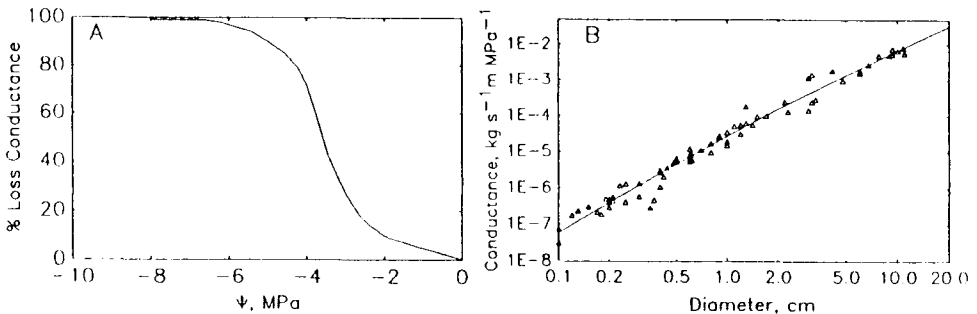


Fig. 2. A. Vulnerability curve for cedar stems. B. Hydraulic conductance *versus* stem diameter for cedar stems.

base joined. A sample numbering scheme for a small branch cut into 11 segments, is shown in Fig. 3. The hydraulic map also catalogued the leaf area attached to each segment, its length and its diameter. The data in Fig. 2B were used to compute a hydraulic resistance of each segment based on its length and diameter. For any given evaporative flux ( $E$ ) the computer model calculated the steady-state water flow rate through each stem segment; from the segment's hydraulic resistance, the model calculated the drop in  $\psi$  across the segment. Starting with input values of soil  $\psi$  and root resistance to water flow, the model could then calculate the  $\psi$  of each segment. The model then used these values of  $\psi$  to calculate the change in stem resistance (inverse conductance) from the vulnerability curves in Fig. 2A. These new resistance values were used to calculate new  $\psi$  values for the same  $E$ . The calculations were repeated until either stable values of hydraulic resistance (reflecting stable levels of embolism) were achieved or until the stem segment was deemed dead and removed from the

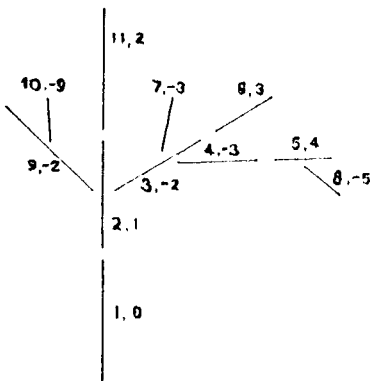


Fig. 3. An illustration of the numbering system used in an 11-segment branch. The first number is the segment number and the second number is the connecting segment number; a minus sign indicates it is a branch.

hydraulic map so that it no longer contributed to the transpiration stream. A segment was deemed dead when its hydraulic conductance had fallen to 5% of its initial value. In Fig. 2A, a 95% loss of conductance also corresponds to a stem  $\psi$  of about  $-5.5$  MPa.

Independent field observations on cedar saplings indicated that  $E$  never exceeded  $1.8 \times 10^{-5} \text{ kg} \cdot \text{s}^{-1} \cdot \text{m}^{-2}$  and that  $\psi$  rarely fell below about  $-2.0$  MPa. The model correctly predicted the observed range of shoot  $\psi$ 's for valid ranges of  $E$ . The vulnerability curve (Fig. 2A) also predicted that, under field conditions, the loss of conductance ought to average about 10%, if shoot  $\psi$ 's never fall much below  $-2.0$ . This percent loss of conductance has been confirmed on field samples (Tyree and Sperry, 1988).

At this point an important question can be asked about the hydraulic sufficiency of cedar stems. Does the vulnerability of cedar stems place a constraint on the maximum rate at which water can flow through the stems? If the embolism cycle (Fig. 1) is unstable, then an increase in water flow rate will result in 'runaway' embolism and stem death. This question can be answered with the model by either increasing the leaf area attached to the stem segments in the model or increasing  $E$  above the maximum rates observed in the field and observing the stability of the embolism cycle. Model calculations that answer this question are illustrated below (see Fig. 4). The solid line in Fig. 4 shows how the average  $\psi$  of all minor branches bearing leaves changed with  $E$ , if there were no loss of conductance by embolism. The dotted line shows the average  $\psi$  of all minor branches when embolism was taken into account. The maximum  $E$  observed under field conditions is marked by an \* near the x-axis. The model predicted that when the loss of conductance in segments exceeded 20–30% then run-

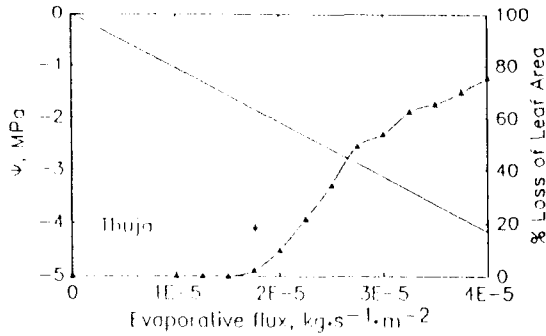


Fig. 4. Model results, see text.

way embolism would occur leading to segment death if  $E$  did not change (that is, stomates did not close). The percentage of all leaf area lost by stem death is shown by the solid line with triangles. When stem death starts (shown by points to the right of the \*), the water balance of the living segments improves. In the dotted line, the  $\psi$  of dead segments is not included in the average for points to the right of the \*. The water flow rate,  $v$   $\text{kg}\cdot\text{s}^{-1}$ , through a stem segment is given by  $E \times A$ , where  $A$  is the area of leaves fed by the segment. Prior to stem death, as  $E$  increases, then  $v$  increases in proportion causing a proportional decrease in  $\psi$ . When stems die as  $E$  increases to the right of the \* in Fig. 4, then  $v$  must decrease because of a proportionally larger decrease in  $A$  as leaves die; consequently the shoot  $\psi$  does not show a further decline for  $E$  values to the right of the \*.

## Materials and Methods

This paper examines the generality of the conclusions drawn from the previous steady-state models (Tyree and Sperry, 1988) by computing the dynamics of embolism development in a non-steady state model. The materials and methods were fully described elsewhere (Tyree, 1988). Briefly, a hydraulic map of a 10 m tall cedar tree was documented. The tree was cut

into 4107 segments. The model took full account of how water storage in stems and leaves affected the tempo of change of  $\psi$  throughout the crown. Tyree (1988) has previously shown that the non-steady-state model correctly predicted field-observed ranges of  $\psi$  from field-measured rates of  $E$ . The water storage capacity of leaves was assigned values obtained from pressure-volume curves and in this paper stem capacitances were assigned a value of  $0.1 \text{ kg}\cdot\text{dm}^{-3}\cdot\text{MPa}^{-1}$ . The following changes in the previous model were made for this paper: 1) computations were started at midnight of d 1 after an adjustment for the level of embolism that might have occurred on previous days; initial values of stem conductance were adjusted upward by 4% for stem segments with diameters between 0.2 and 1.0 cm and by 8% for stem segments of  $<0.2$  cm in diameter; 2) a record was kept of the minimum value of  $\psi$  attained by each segment as time progressed in the calculations; 3) the value of stem conductance used as time progressed was based on the minimum  $\psi$  value recorded according to the vulnerability curve in Fig. 2A.

## Results

The dynamics of embolism development and loss of leaf area over a 3 d period is illustrated in Fig. 5. The average  $E$  versus time is shown in the upper panel. The  $E$  for each compass quadrant actually differed according to Tyree (1988, Fig. 1d). The resulting stem  $\psi$ 's plotted in the upper panel are means for stems of  $<0.1$  cm dia-

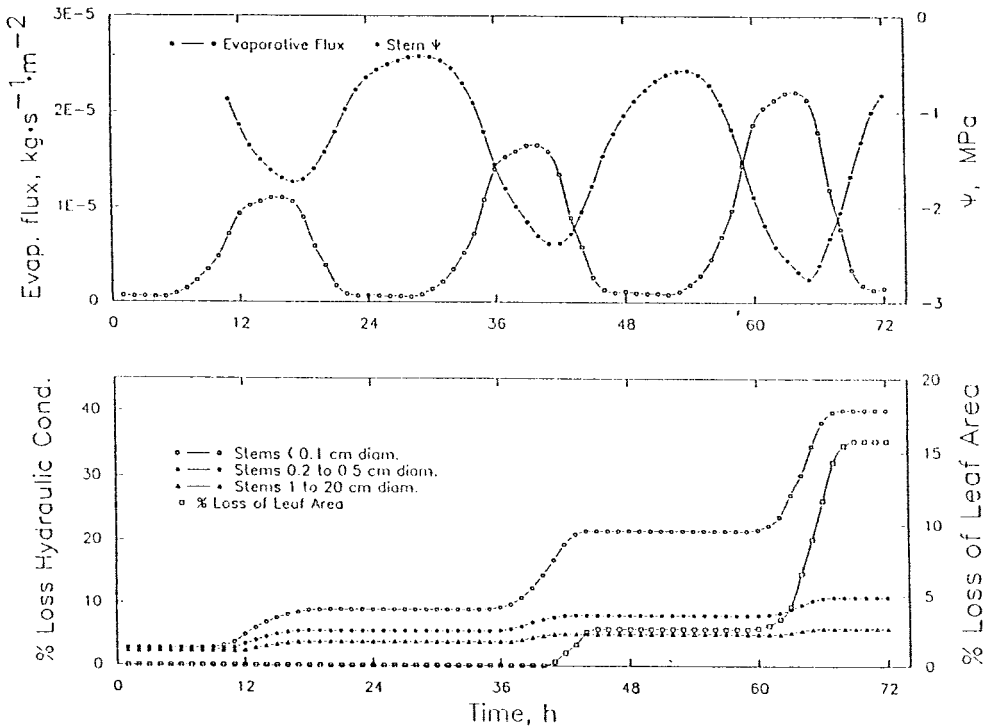


Fig. 5. Results of the non-steady-state model for the dynamics of embolism development in a 10 m cedar tree. See text for details.

meter in the mid-crown of the cedar tree. On d 1 the  $E$  values used were those on a typical sunny day (Tyree, 1988); on d 2 and 3 the values of  $E$  were 1.5x and 2.0x higher, respectively. After the 1st d (with typical  $E$  values), the loss of conductance was about 9 and 5% in minor branches (<0.1 cm in diameter) and larger branches (between 0.2 and 0.5 cm in diameter), respectively. These changes were approximately equal to the amount by which conductances had been increased prior to the start of calculations (see Materials and Methods). No runaway embolism or leaf loss was predicted.

Higher evaporation rates caused runaway embolism. By the end of d 2, when  $E$  peaked 1.5x higher than on d 1, the loss of conductance in minor branches had

increased to 22% and 3% loss of leaf area had occurred due to runaway embolism. By the end of d 3, when  $E$  peaked at 2.0x higher than on d 1, the loss of conductance of minor branches reached 40% with a 16% loss of leaf area. The model predicted runaway embolism only in branches of <0.3 cm diameter. The frequency histogram (see Fig. 6) shows the distribution of embolism in branches of <0.3 cm diameter at midnight on d 3 (72 h). The bimodal pattern indicates 2 populations of stems. Those with <30% loss of conductance and those with >90%. There are a few stragglers between, but it can be shown that the stragglers quickly move to the >90% category, when the evaporation rates of d 3 are repeated for 2 more days. After these additional 2 d, the loss of leaf

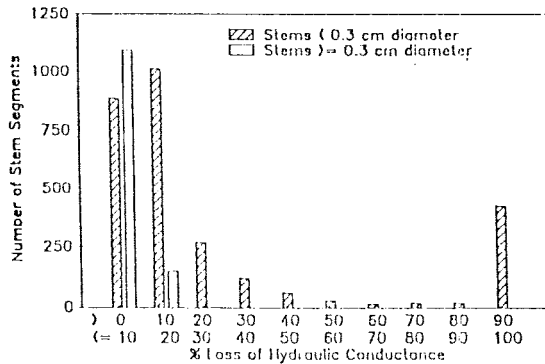


Fig. 6. Frequency histogram for the distribution of embolism after 3 days of  $E$  as in Fig. 5.

area has increased to 18.3% and the minimum average stem  $\psi$  has eased off to  $-2.39$  MPa from  $-2.76$  MPa shown in Fig. 5 at 65 h.

## Discussion and Conclusion

The results of the non-steady-state and steady-state models were qualitatively quite similar. When  $E$  exceeded a critical threshold value, then runaway embolism caused a patchwork dieback in minor twigs as predicted by the plant segmentation hypothesis. Normal rates of evaporation in cedar closely approached this critical level. The quantitative differences between models were in the direction expected. In the non-steady-state model, the values of  $E$  peaked at 1.8, 2.4, 2.6 and  $2.8 \times 10^{-5} \text{ kg} \cdot \text{s}^{-1} \cdot \text{m}^{-2}$  on the north, east, west and south quadrants of the crown, respectively. Using these  $E$  values in a steady-state model led to a predicted loss of leaf area of about 29% over the entire crown. In the non-steady-state model, the loss of leaf area was less (18%). As expected, water storage capacity of stems and leaves reduced the extremes in  $\psi$  at-

tained in minor branches compared to that predicted by the steady-state model with a consequent reduction in loss of leaf area.

It is rare to find individual trees that suffer significant leaf loss due to drought. This is presumably because stomates close and reduce  $E$  before runaway embolism causes leaf loss. When the steady-state model was modified to allow for stomatal closure at  $\psi = -2.0$  MPa, then runaway embolism was not predicted. The value of the model (without stomatal regulation), is that it shows that, due to embolism, cedar operates near the point of catastrophic xylem failure. Similar conclusions (Tyree and Sperry, 1988) have been drawn for maple (*Acer saccharum*) and 2 tropical species: red mangrove (*Rhizophora mangle*) and a moist forest relative (*Cassipourea elliptica*). It is common to see a patchwork pattern of brown foliage in cedar trees. This might be due to runaway embolism in the summer or due to winter dehydration of the sapwood which, if not reversed in spring, would lead to runaway embolism at modest evaporation rates in spring.

Runaway embolism might be a potential threat for all woody species. If so, this would suggest a strong selective process

for a number of diverse morphological and physiological properties that keep the water relation of the species in proper balance. These morphological features include: leaf area supported per unit stem area, stomatal diameter, stomatal frequency (number per unit area) and xylem structure (small *versus* large conduits). One can speculate that xylem structure (tracheids *versus* vessels) might be much less genetically mutable than the genetics that determine leaf size and number, stomatal size, frequency and physiology. A tree cannot improve its competitive status with regard to competition for light and net assimilation through any process that would increase  $E$  without changing the less mutable xylem morphology. Typical field values of  $E$  for cedar are about one tenth that of broadleaf species. Also, cedar supports slightly larger leaf areas per unit stem area than do broadleaf species. This can be explained in terms of 2 factors that make cedar sapwood less hydraulically sufficient than that of broadleaf species: 1) the vulnerability of cedar to cavitation is higher than that of many broadleaf species (Tyree and Sperry, 1989); and 2) the hydraulic conductance per unit sapwood area in cedar is much less than that of broadleaf species.

The hydraulic sufficiency of trees may provide new insights into the evolution of the morphology, physiology and ecophysiology of woody plants. For example, up until now, it had been presumed that stomatal closure under water stress occurred primarily to prevent desiccation damage to the biochemical machinery of the photosynthetic system. It is now clear that another important role of stomatal regulation is to prevent runaway embolism, while pressing water conduction through stems

to their theoretical limit of hydraulic sufficiency. Trees must evolve mechanisms to keep an appropriate balance for carbon allocation between leaves (which increase evaporative demand) and stems (which supply the demand for water evaporated from the leaves).

## References

- Bailey I.W. (1916) The structure of the bordered pits of conifers and its bearing upon the tension hypothesis of the ascent of sap in plants. *Bot. Gaz.* 62, 133-142
- Dixon H.H. (1914) *In: Transpiration and the Ascent of Sap in Plants.* MacMillan, London
- Ewers F.W. & Zimmermann M.H. (1984a) The hydraulic architecture of balsam fir (*Abies balsamea*). *Physiol. Plant.* 60, 453-458
- Ewers F.W. & Zimmermann M.H. (1984b) The hydraulic architecture of eastern hemlock (*Tsuga canadensis*). *Can. J. Bot.* 62, 940-946
- Sperry J.S., Donnelly J.R. & Tyree M.T. (1987) A method for measuring hydraulic conductivity and embolism in xylem. *Plant. Cell Environ.* 11, 35-40
- Tyree M.T. (1988) A dynamic model for water flow in a single tree. *Tree Physiol.* 4, 195-217
- Tyree M.T. & Sperry J.S. (1988) Do woody plants operate near the point of catastrophic xylem dysfunction caused by dynamic water stress? Answers from a model. *Plant Physiol.* 88, 574-580
- Tyree M.T. & Sperry J.S. (1989) Vulnerability of xylem to cavitation and embolism. *Annu. Rev. Plant Physiol.* 40, 19-38
- Tyree M.T., Graham M.E.D., Cooper K.E. & Bazos L.J. (1983) The hydraulic architecture of *Thuja occidentalis* L. *Can. J. Bot.* 61, 2105-2111
- Zimmermann M.H. (1978) Hydraulic architecture of some diffuse porous trees. *Can. J. Bot.* 56, 2286-2295
- Zimmermann M.H. (1983) *In: Xylem Structure and the Ascent of Sap.* Springer-Verlag, Berlin, pp. 143